Kathmandu University Journal of Science, Engineering and Technology, Vol. 19, No. 3, December 2025

Kathmandu University
Journal of Science, Engineering and Technology

Study of quasi-periodic oscillation in X-ray lightcurve of BL Lac using Swift/XRT

Nabin Bhusal* , Manil Khatiwada , and Bishal Khanal

Central Department of Physics, Tribhuvan University, Kritipur, Nepal.

Abstract

We analyzed 17 years (2005–2022) of X-ray time series data from the BL LAC object, a type of active galactic nucleus, using open data from the Neil Gehrels $Swift$ Observatory. Data with exposure times exceeding 1000 seconds in photon-counting (PC) and windowed timing (WT) modes were processed using HEASoft, software. Rapid XRT data analysis revealed quasi-periodic oscillation (QPO) in BL LAC, a bright source potentially influenced by complex motions, such as those of a supermassive binary black hole system. We employed power spectral density (PSD), epoch folding, and autocorrelation function (ACF) methods to investigate periodicity. The light curve exhibited red noise characteristics, and frequency domain analysis confirmed a 1.593 hour QPO. These findings contribute to understanding the variability and potential binary nature of BL LAC objects.

Keywords: X-ray variability; $Swift$ observatory; Timing analysis; Binary black holes.

1. Introduction

Astronomy studies the origin and evolution of celestial bodies and high-energy phenomena, including black holes and active galactic nuclei [1, 2]. In the early 20th century, astronomy was limited to the optical band. The emergence of radio astronomy in the 1950s, driven by advances in electromagnetic wave technology, enabled the discovery of quasars, pulsars, and radio galaxies [3, 4]. Technological developments in rockets, balloons, and satellites enabled X-ray observations above Earth's atmosphere, essential due to atmospheric attenuation of low-energy X-rays [5, 6]. The first X-ray image of the Sun was captured on April 19, 1960, using a pinhole camera aboard an Aerobee-Hi rocket. In 1962, the first extra-solar X-ray source was detected, marking a breakthrough due to the distinct observational techniques required in X-ray astronomy. Goddard's X-ray program began with balloon experiments in 1965, followed by sounding rocket missions in the 1970s and orbiting observatories thereafter [7]. A milestone was the 1975 X-ray image of the Virgo Cluster. Major X-ray missions such as HEAO, EXOSAT, Ginga, RXTE, ROSAT, ASCA, BeppoSAX, and Chandra have advanced the field. These observations help decode high-energy emission mechanisms and fundamental cosmic processes. Today, AGNs are explored across the full spectrum-from radio to TeV γ-rays-supported by open-access data from observatories like $Swift$ [8]. AGN are extremely luminous regions at galaxy centers, powered by accretion onto supermassive black holes. Emitting across the entire electromagnetic spectrum, AGN includes quasars, blazars, Seyfert galaxies, and radio galaxies. Their emission depends on energy output mechanisms, often featuring powerful, collimated jets perpendicular to the accretion disk [6, 9]. The classification in Table 1 is based on their optical and ultraviolet spectra.

Blazars, first identified in 1929 and unified in 1980, are AGNs with jets aimed at Earth. They show rapid variability, high non-thermal emission, and X-rays from the inner accretion disk, powered by a supermassive black hole [11]. Blazars show a two-peaked SED: the low-energy peak (UV–soft X-rays) from synchrotron radiation, and the high-energy peak (X-rays–γ-rays) from inverse Compton or hadronic processes [12]. Blazar variability spans wide temporal and spatial scales. A 1996 study reported variability amplitude correlating with redshift and anticorrelating with luminosity. However, later observations of 15 blazars found no clear correlation with either [13]. Variability in the V band is generally larger than in the R band, though exceptions exist, with some cases showing equal or greater variability in the R band. This suggests that the assumption of systematically larger variability at higher frequencies may not always hold. Recent research also indicates that blazar variability can be quasi-periodic [13, 14, 15]. BL Lacertae is an unusual type of AGN of BL LAC objects which have rapid variability and high polarization. According to radio loudness, BL Lacertae is AGN of radio-loud source. There are around 40 BL LAC objects known, one is BL Lacertac which is bright source [16].

BL Lacertae is located about 950 million light-years from Earth, which is the most energetic type of black-hole-powered galactic core. Supermassive black holes, about 200 million times the mass of our Sun in the case of BL LAC – in these galaxies' cores power jets of electrically charged particles and intense radiation [17]. Initially, this source at that time was classified as an LBL in TeVCat but because of the BL LAC's characteristics, it has been updated to an IBL. This update was based on its classification in the Fermi 2^{nd} AGN Catalog [18]. BL LAC is the Source Type of IBL and has the other name 1ES 2200+420 and TeVCat Name TeV J2202+422 with (z= 0.069) R.A. (J2000): 22h 02m 43.3s and 4. (J2000): 42d 16' 40" [19]. Nowadays, the source has been extensively studied in a broad range of the electromagnetic spectrum by using several instruments whereas featureless BL LAC objects including BL Lacertae or BL LAC have been neglected for several years.

$Swift$ is a 2004 space telescope for rapid GRB detection and

*Corresponding author. Email: nabinbhusal25@gmail.com

Table 1: Classification of AGN [10].

Type	Subtype	Abbreviation	Properies
Type 1	1. Steep spectrum radio-quasars	1. SSRQ	1. Quasar with steep radio spectrum($\alpha > 0.5$)
	2. Quasi-steller object	2. QSO	2. Distant source with braod lines
	3. Flat-spectrum radio quasar	3. FSRQ	3. Quasar with flat radio spectrum($\alpha < 0.5$)
	4. Seyfert 1	4. Sy1	4. Broad + narrow emission lines
Type 2	1. Fanaroff-Riley radio galaxy	1. FR1	1. Low-power, core-bright radio galaxy
	2. Fanaroff-Riley radio galaxy	2. FR2	2. High-power, lobe bright radio galaxy
	3. Seyfert 2	3. Sy2	3. Only narrow line emission
Type 3	1. BL Lacertae	1. BL LAC	1. Featureless optical continuum, weak lines
	2. Optically violent variable AGN	2. OVV	2. Highly variable, polarized, apparent superluminal motion

study across 0.002–150 keV using BAT, XRT, and UVOT [20]. The $Swift$ X-Ray Telescope (XRT) is a sensitive CCD-based imaging spectrometer designed to study GRB afterglows, providing spectra, light curves, and localization within ~2 arcsec [21, 22]. The Swift/XRT parameters are given in Table 2.

Table 2: Swift/XRT parameters [23].

XRT Parameter	Value
Telescope	JET-X Wolter 1
Energy range	0.2-10 keV
Detector	E2V CCD-22
Detector format	600 x 600 pixels
Pixel size	40 μm × 40 μm
Readout modes	Image (IM) mode, Photodiode (PD) mode, Windowed Timing (WT) mode, and Photon-counting (PC) mode
Pixel scale	2.36 arcseconds/pixel
Field of view	23.6 × 23.6 arcminutes
PSF	18 arcseconds HPD 1.5 keV, 22 arcseconds HPD 8.1 keV
Position accuracy	3 arcseconds
Time resolution	0.14 ms, 1.8 ms, or 2.5s
Energy range	0.2-10 keV
Energy resolution	140 eV 5.9 keV (at launch)
Effective area	110 cm^2 @ 1.5 keV

Numerous studies have searched for quasi-periodic oscillations (QPOs) in blazars across optical, radio, X-ray, and γ-ray bands. Early photographic monitoring of OJ 287 and BL Lacertae using the Scargle periodogram yielded only 50% significance for optical periodicity [24, 25]. Radio and optical campaigns by WEBT over 30 years found ~8 yr periodicity in radio hardness ratios, with weaker optical signatures using DFT, ACF, and SF techniques [26, 27]. RXTE ASM data (1.5–12 keV) for 24 blazars revealed a 313 ± 12-day QPO in BL LAC's X-ray light curve via structure function and DCF analysis [28]. XMM-Newton archival observations also indicate non–yearly quasi-periods in BL LAC using WWZ and LSP methods [29]. Fermi γ-ray sky analyses identified ~680-day cycles in BL LAC and PG 1553+113 with generalized Lomb–Scargle periodograms [30]. Combined optical (AAVSO) and radio (OVRO, UMRAO) data from 1970–2018 exhibit ~9 yr optical and ~8 yr radio QPOs for BL LAC [31]. Recent Fermi studies of bright γ-ray blazars cast doubt on robust year-long QPOs amid red-noise, underscoring the need for rigorous verification [32]. These mixed results motivate our targeted timing analysis of Swift-XRT data to confirm X-ray QPOs in BL LAC.

2. Methodology

This study utilizes power spectral density and epoch folding methods to detect and verify QPOs. Data analysis requires HEASoft, software package (version 6.30), which includes Swift-specific tools, standard FTOOLS, and XANADU packages. Installation follows the verified procedures available online, and the calibration database (CALDB v1.02) must be locally installed for proper data calibration. Once the software setup is complete, $Swift$ data can be downloaded and processed. Public Swift-XRT data, including exposure times, are cataloged in the Swift-XRT master catalog, which provides high-level data and archive access for each observation ID. For this study of BL Lacertae, observations with exposure times exceeding 1000 seconds were downloaded, spanning 17 years from October 28, 2005, to March 12, 2022. A total of 386 observation IDs were obtained, with 311 in window timing (WT) mode and 75 in photon counting (PC) mode; one WT observation (ID 00030720160) was excluded due to errors.

Swift-XRT data were processed using the HEASARC pipeline. Source and background regions were defined in SAOImage DS9 (RA=330.680, DEC=42.277). A 20-pixel radius was used for source extraction in both WT and PC modes; background regions were 40 pixels (PC) and 20 pixels (WT). High-level products were generated with xrtproducts. Light curves were background-subtracted using lcmath and binned into .flc files via lcurve. For pile-up affected data, the inner radius was estimated using ximage, and an annular region (inner radius from analysis, outer radius 20 pixels) was defined in DS9 as shown in Fig.1. Background regions were the same as in non-pile-up cases. Pile-up occurs when multiple photons are recorded as one event. It is significant above ~0.5 counts (PC) or ~100 counts (WT). In this study, no pile-up was found in PC mode, though 33 observations near the threshold were checked.

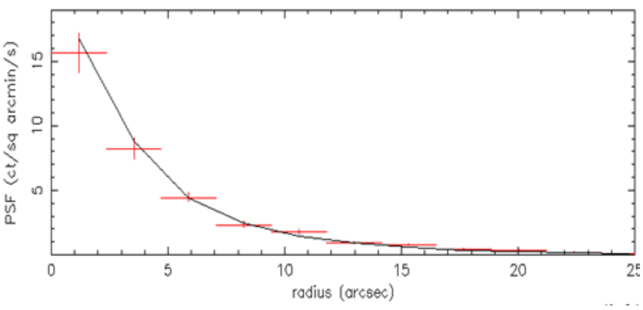

Figure 1: Radial profile of the point spread function (PSF) showing the effect of pile-up. The plot displays PSF intensity versus radius. The central deficit relative to the model curve indicates photon pile-up, where multiple photons are registered as a single event. This profile is used to define an annular extraction region that excludes the piled-up core for accurate spectral and timing analysis.

3. Results and discussion

3.1. The light curve

The analyzed light curve of the source blazar BL LAC is given in Fig. 2. The light curve clearly shows the periodic modulation when the time in seconds is 2.24208×10^8, 3.482635×10^8, 4.83635×10^8, the count rate is above the average count rate. Standard deviation is 0.28897, average count per second is 0.44311, minimum count is 0.3307, and maximum count per second is 1.8190. The start time and end time are given in the efold graph.

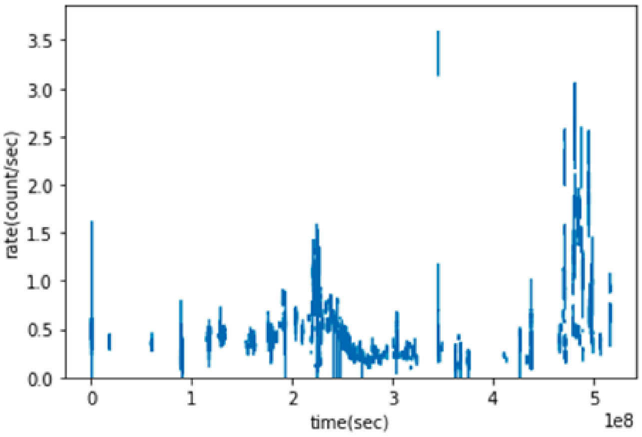

Figure 2: X-ray light curve showing source variability over time. The count rate (counts/sec) varies with time (sec), indicating intrinsic brightness fluctuations of the source.

The autocorrelation of the graph of the light curve is given by Fig. 3, which shows the autocorrelation signals for the blazar BL LAC. The horizontal axis shows the time delay as calculated from the arm length difference. The autocorrelation function is mostly affected by pulse rate. The graph of Fig. 3 has a different spatial position. Different spatial positions in the autocorrelation graph correspond to different time delays. By the graph of the autocorrelation function different spatial positions of autocorrelation are seen i.e., there are some time delays in light curve of Fig. 2. There is positive and negative type of autocorrelation which means that the process is completely uncorrelated but serially correlated in time. The light curve process is a red noise process. Here the search of QPO of such noise process i.e., having zero meaning and finite variance in the autocorrelation function serially correlated in time. For search period, the time obtained from the maximum power of frequency is period of oscillation. Also, if the power spectrum weighed towards low frequency without preferring single point it is red noise [33].

3.2. Power spectrum density (PSD)

The power spectrum density of a signal is its power distribution over its frequency. A binary process might cause the power spectrum line to fluctuate. The power spectrum may also be used to determine the amount of noise present in broadcasts. To obtain PSD, the amplitude of the FFT is multiplied by its complex conjugate and normalized to the frequency bin width. Power spectral density characterizes a stationary random process in the frequency domain. Power spectrum is discrete-time Fourier transform (DTFT) of the correlation process. For power spectra s(f) and correlation processes r[k], they are changeable by the DTFT as,

$$s(f) \leftrightarrow r[k] \tag{1}$$

$$s(f) = \sum_{k=-\infty}^{\infty} r[k] e^{-jkf} \tag{2}$$

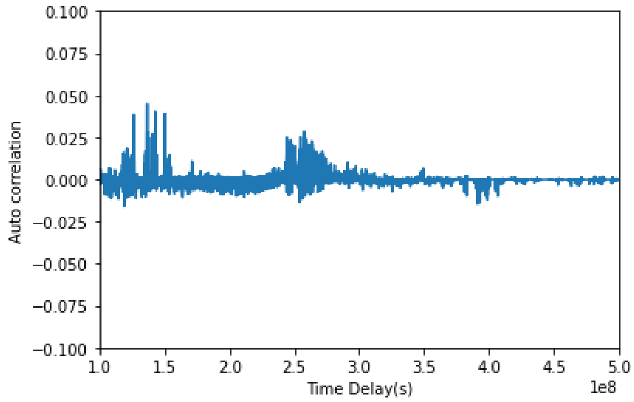

Figure 3: An autocorrelation plot. The x-axis represents the time delay, while the y-axis shows the autocorrelation coefficient, indicating the strength and direction of correlation of the signal with itself at various delays. This plot helps identify hidden patterns and periodicities within the time series data.

$$r[k] = \frac{1}{2\pi} \int_{-\pi}^{\pi} s(f) e^{jkf} df \tag{3}$$

The unit of power spectrum density is power/Hz. As the name implies, the Fast Fourier Transform (FFT) is an algorithm that determines the Discrete Fourier Transform of an input significantly faster than computing it directly. FFT reduces the number of computations needed for a problem of size N from O(N^2) to O(NlogN). In equation 1 FFT can also do the work as DTFT. The estimation of the square of the value is done by

$$P(\vartheta) = \frac{T}{n^2 F^2} (|\sum_{j=1}^{n} x(t_j) e^{-2\pi\vartheta t}|)^2 \tag{4}$$

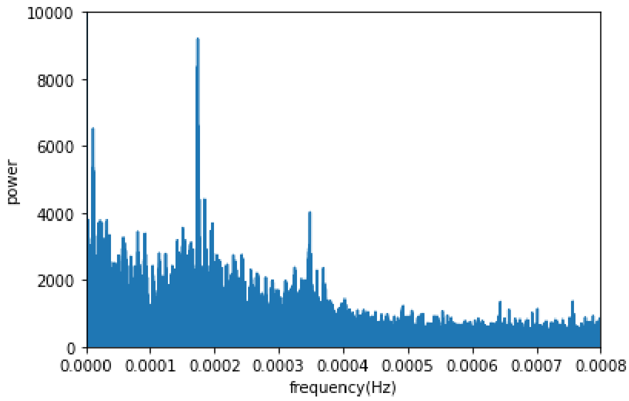

Figure 4: Power spectral density of BL LAC object by Swift observations, with frequency (Hz) on the x-axis and corresponding power on the y-axis, highlighting maximum power at 9198.47 Hz.

After giving the file in XRONOS, it read all information like start time, stop time, bin time, etc. By passing with default windows, a 300-bin time was given to make only one interval of data. Wdata obtained from that was plotted as Fig. 4. Because of the periodic process, the power spectrum line fluctuates over frequency for power. To make clear the time of spectral analysis, negative binning was done.

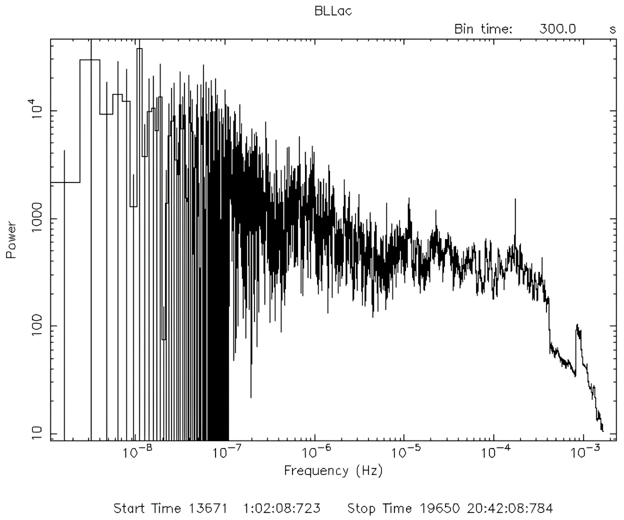

Figure 5: Power spectral density of Swift XRT data for BL LAC object, analyzed to search for quasi-periodic oscillations (QPOs), with a bin time of 300.0 seconds.

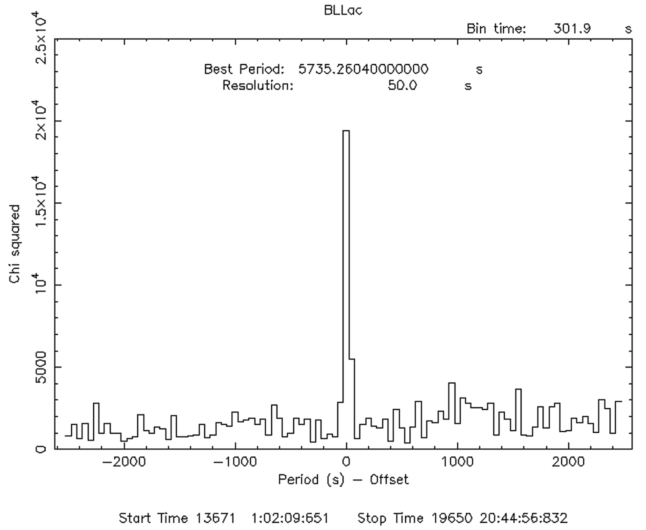

Figure 6: Efsearch graph generated by XRONOS for the Swift XRT light curve of the BL LAC object. The chi-squared values are plotted against trial periods, showing a prominent peak at 5735 seconds, which suggests the presence of quasi-periodic oscillation (QPO) at this period.

3.3. The efsearch

Calculating χ^2 in epoch folding, for N_b phase bins is done by,

$$\chi^2 = \sum_{i=1}^{N_b} \frac{(x_i - x)^2}{\sigma_i^2} \tag{5}$$

χ^2 is dependent on the time series and pulse shape. To make noise-free signals, the error of the Gaussian frequency of non-sinusoidal oscillation should be taken in epoch folding. The period as described by Fourier component is described as,

$$\sigma_p^2 = \sum_{k=-\infty}^{\infty} \frac{\sigma_{total}^2}{\pi^2 T^2 N} \frac{P^2}{\sum_{k=-\infty}^{\infty} k^2 A_k^2} \tag{6}$$

In this work, epoch folding was done using the efsearch task from the XRONOS package in HEASoft, FTOOLS- the graph is in Fig. 6. It automatically calculates the harmonic chi-square (χ^2) to find the best period by maximizing the χ^2 value from the light curve. The period estimated from the power spectral density (PSD), about 19 seconds, was used. This helped generate phase bins over an interval of around 300 seconds. Since XRONOS only accepts integers, the number of bins per period was given as an integer. A resolution of 50 seconds was used, and 128 trial periods were tested.

3.4. efold

A specific or estimated period is used to fold the data and create a phase-folded light curve. This is done using the efold task, with the hidden parameter perfo set to 1, meaning the period is given in days. The light curve file, along with the default window epoch and period (as used in efsearch), is provided. The nphase parameter defines the number of phase bins per period, which sets the resolution of the folded profile. The resulting plot of count rate versus phase is saved, and the graph is shown in the figure as Rate vs Phase. From Fig. 4 and 5, power spectrum density graph, it was obtained that, for maximum power 9198.47, the period is 5735.26 sec. Which is 1.593 hours. Red noise data should be epoch folded with time [33]. So efsearch was done. By efsearch, Fig. 6 gives best period of 5735.26 seconds is 1.593 hours for the observation of blazar BL LAC using the epoch folding search. It verifies the time that was obtained from PSD graph. By this graph we obtain the phase characters, using them phase folded light curved was made. Which shows the very well-defined folded phase. Which is folded to 5735.26 second in Fig. 7. Hence QPO of 5735.26 second is 1.593 hours is seen in observation of BL Lac.

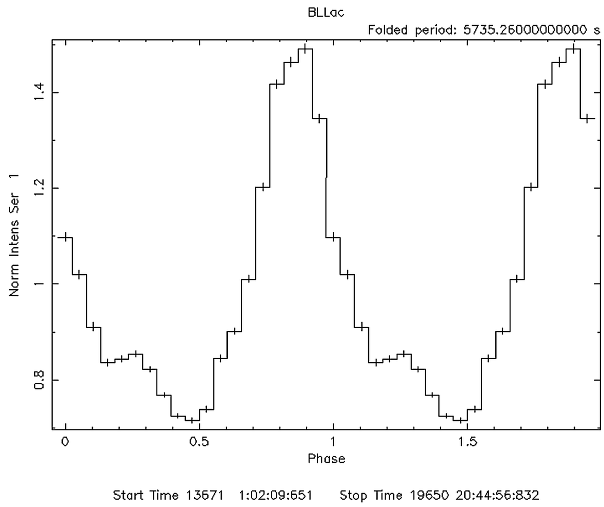

Figure 7: Phase-folded light curve of the BL LAC object derived from Swift XRT data, folded over a period of 5735.26 seconds, showing normalized intensity variations across two (phase 0 to 2), with observations spanning from 136771 1:02:09.651 to 136950 20:44:56.832.

In PSD curve the first maximum power is of epoch blast. From the second pick of power spectrum the Quasi-periodicity of 5735.26 sec, which is 1.593 hours. This Quasi-periodicity time is verified by epoch folding method, which gives clear pick in zero phase which is shown in Fig. 6. This phase gives the phase folded light curve as in Fig. 7.

4. Conclusion

A binary black hole (BH) system may cause fluctuations in the power spectrum due to frequency shifts [34]. Black hole and neutron star X-ray binary systems are known to exhibit quasi-periodic oscillations (QPOs) in their X-ray flux. If the QPOs observed in BL LAC objects were due to a supermassive binary black hole (SBBH) system, this could conflict with the upper limits on the gravitational wave background set by pulsar timing array experiments. This suggests the difficulty of confidently associating QPOs in BL LAC objects with SBBHs [35].

QPOs in blazars may also arise from jet emissions, possibly driven by perturbations near the black hole [28]. Therefore, current evidence is insufficient to conclusively classify BL LAC as a binary system. Moreover, low-frequency QPOs often appear as stochastic variations in spectral analysis, which reduces the reliability of any associated confidence level in the power spectrum density (PSD) graph [30].

In one relevant study [28], performed a structure-function analysis using over 12 years of X-ray data from the Rossi X-Ray Timing Explorer (RXTE) All-Sky Monitor for 24 blazars in the 1.5–12 keV energy range. Their findings did not support the one-year QPO claims previously made by Rani et al. If a true QPO with a period of roughly one year existed in a blazar like BL LAC, the PSD should show a significant peak at the corresponding frequency. However, in our case, we observe a much shorter QPO timescale. This may suggest that, if a binary system is present, the black holes are in extremely rapid orbital motion. Thus, the detection of a QPO in a blazar could hint at the presence of a binary supermassive black hole system. However, before concluding such a scenario, the binary model must also be able to explain other physical and observational properties of the source consistently.

Author contributions

Nabin Bhusal and Manil Khatiwada contributed to the conception of the study, data analysis, interpretation of results, and preparation of the manuscript. Bishal Khanal contributed to the manuscript through writing assistance, editing, and preparation of the final draft.

Acknowledgments

The authors acknowledge the Swift mission team for providing the observational data used in this study. This research has made use of data supplied by the High Energy Astrophysics Science Archive Research Center (HEASARC), operated by the NASA Goddard Space Flight Center.

References

[1] Unsöld A & Baschek B. *Classical Astronomy and the Solar System*. Springer Berlin Heidelberg, Berlin, Heidelberg (1991). ISBN 978-3-662-02681-6, pp. 3–73. https://doi.org/10.1007/978-3-662-02681-6_2.

[2] Madejski G. *Black Holes in active galactic nuclei*. Springer Berlin Heidelberg (2002). ISBN 9783642557392, pp. 36–45. https://doi.org/10.1007/978-3-642-55739-2_4.

[3] Khatiwada M, Bhusal N, Khanal B & Rana K, Detection of quasiperiodic oscillation in X-ray light curve of Blazar OJ 287 using SWIFT/XRT, *Himalayan Physics*, 12 (2025) 24–40. https://doi.org/https://doi.org/10.3126/hp.v12i1.78399.

[4] Hey J S. *The evolution of radio Astronomy*, vol. 1. Science History Publications, New York (1973). URL https://archive.org/details/evolutionofradio0000unse_o3q7.

[5] Bhusal N, Kunwar M & Dhital N, Statistical signatures of Gamma-ray burst 221009A in X-ray observations, *Research in Astronomy and Astrophysics*, 25(7) (2025) 075006. ISSN 2397-6209. https://doi.org/10.1088/1674-4527/adda7f.

[6] Beall J H, A review of astrophysical jets, *Acta Polytechnica CTU Proceedings*, 1(1) (2014) 259–264. ISSN 2336-5382. https://doi.org/10.14311/app.2014.01.0259.

[7] Shields G, A brief history of active galactic nuclei, *Publications of the Astronomical Society of the Pacific*, 111(760) (1999) 661–678. ISSN 1538-3873. https://doi.org/10.1086/316378.

[8] Sullivan W T. *The early Years of Radio Astronomy: reflections fifty years after Jansky's Discovery*. Cambridge University Press, Cambridge, England (2005). ISBN 9780511564956. https://doi.org/10.1017/cbo9780511564956.

[9] Rees M J, Black Hole models for active galactic nuclei, *Annual Review of Astronomy and Astrophysics*, 22(1) (1984) 471–506. ISSN 1545-4282. https://doi.org/10.1146/annurev.aa.22.090184.002351.

[10] Urry C M & Padovani P, Unified schemes for radio-loud active galactic nuclei, *Publications of the Astronomical Society of the Pacific*, 107 (1995) 803. ISSN 1538-3873. https://doi.org/10.1086/133630.

[11] Impey C, Quasars, Blazars, and the Gamma-ray sky, *Astronomical Journal*, 112 (1996) 2667. ISSN 0004-6256. https://doi.org/10.1086/118211.

[12] Donato D, Ghisellini G, Tagliaferri G & Fossati G, Hard X-ray properties of Blazars, *Astronomy and Astrophysics*, 375(3) (2001) 739–751. ISSN 1432-0746. https://doi.org/10.1051/0004-6361:20010675.

[13] Massaro E & Trevese D, A statistical bias in the spectral index - flux correlation of AGNs, *Astronomy and Astrophysics*, 312 (1996) 810–814.

[14] Ghosh K K, Ramsey B D, Sadun A C & Soundararajaperumal S, Optical variability of Blazars, *The Astrophysical Journal Supplement Series*, 127(1) (2000) 11–26. ISSN 1538-4365. https://doi.org/10.1086/313313.

[15] Bhatta G, Radio and γ-ray variability in the BL Lac PKS 0219-164: detection of quasi-periodic oscillations in the radio light curve, *The Astrophysical Journal*, 847(1) (2017) 7. ISSN 1538-4357. https://doi.org/10.3847/1538-4357/aa86ed.

[16] Weiler K W & Johnston K J, A study of BL Lacertae objects, *Monthly Notices of the Royal Astronomical Society*, 190(2) (1980) 269–285. ISSN 1365-2966. https://doi.org/10.1093/mnras/190.2.269.

[17] Boettcher M, Modeling the emission processes in Blazars, *Astrophysics and Space Science*, 309(1) (2006) 95–104. https://doi.org/10.48550/ARXIV.ASTRO-PH/0608713.

[18] Ackermann M, Ajello M, Atwood W B, Baldini L, Ballet J, Barbiellini G, Bastieri D, Bechtol K, Bellazzini R, Berenji B, Blandford R D, Bloom E D, Bonamente E, Borgland A W, Brandt T J, andS J B, others & Zimmer, Fermi-lat observations of the diffuse γ-ray emission: Implications for Cosmic rays and the interstellar medium, *The Astrophysical Journal*, 750(1) (2012) 3. ISSN 1538-4357. https://doi.org/10.1088/0004-637x/750/1/3.

[19] Albert J, Aliu E, Anderhub H, Antoranz P, Armada A, Baixeras C, Barrio J A, Bartko H, Bastieri D, Becker J K, Bednarek W, Berger K, andJ C B, others & Zapatero, Discovery of very high energy γ-ray emission from the low-frequency-peaked BL Lacertae object BL Lacertae, *The Astrophysical Journal*, 666(1) (2007) L17–L20. ISSN 1538-4357. https://doi.org/10.1086/521550.

[20] Sakamoto T, Barthelmy S D, Barbier L, Cummings J R, Fenimore E E, Gehrels N, Hullinger D, Krimm H A, Markwardt C B, Palmer D M, Parsons A M, Sato G, Stamatikos M, Tueller J, Ukwatta T N & Zhang B, The first Swift BAT Gamma-ray burst catalog, *The Astrophysical Journal Supplement Series*, 175(1) (2008) 179–190. ISSN 1538-4365. https://doi.org/10.1086/523646.

[21] Breeveld A A, Landsman W, Holland S T, Roming P, Kuin N P M & Page M J, An updated ultraviolet calibration for the SWIFT/UVOT (2011) 373–376. https://doi.org/10.48550/ARXIV.1102.4717.

[22] Pagani C, Morris D C, Racusin J, Grupe D, Vetere L, andF M S, others & Tamburelli. Characterization and evolution of the Swift X-ray telescope instrumental background. In: X-Ray U V & Space G R, eds., *UV, X-Ray, and Gamma-Ray Space Instrumentation for Astronomy XV*, vol. 6686. SPIE (2007 2007). ISSN 0277-786X, p. 668609. https://doi.org/10.1117/12.734398.

[23] Gehrels N, Ramirez-Ruiz E & Fox D B, Gamma-ray bursts in the Swift era, *Annual Review of Astronomy and Astrophysics*, 47(1) (2009) 567–617. ISSN 1545-4282. https://doi.org/10.1146/annurev.astro.46.060407.145147.

[24] Carini M, Miller H, Noble J & Goodrich B, The timescales of the optical variability of Blazars. ii - AP Librae, *The Astronomical Journal*, 101 (1991) 1196. ISSN 0004-6256. https://doi.org/10.1086/115756.

[25] Marchenko S G, Hagen-Thorn V A, Yakovleva V A & Mikolaichuk O V, Search for periodicity in the brightness variations of the active extragalactic objects BL Lac, OJ 287, and 3C 120, *Blazar Continuum Variability*, 110 (1996) 105. URL https://www.aspbooks.org/a/volumes/article_details/?paper_id=13408.

[26] Neshpor Y I, Chalenko N N, Stepanian A A, Kalekin O R, Jogolev N A, Fomin V P & Shitov V G, Bl Lac: A new ultrahigh-energy gamma-ray source, *Astronomy Reports*, 45(4) (2001) 249–254. https://doi.org/10.48550/ARXIV.ASTRO-PH/0111448.

[27] Villata M, Raiteri C, Aller H, Aller M, Teräsranta H, Koivula P, Wiren S, Kurtanidze O, Nikolashvili M, Ibrahimov M & Papadakis I, The WEBT campaigns on BL Lacertae: Time and cross-correlation analysis of optical and radio light curves 1968–2003, *Astronomy & Astrophysics*, 424(2) (2004) 497–507. ISSN 1432-0746. https://doi.org/10.1051/0004-6361:20040439.

[28] Rani B, Wiita P J & Gupta A C, Nearly periodic fluctuations in the long-term x-ray light curves of the Blazars AO 0235+164 and 1ES 2321+419, *The Astrophysical Journal*, 692(2) (2009) 2170–2178. ISSN 1538-4357. https://doi.org/10.1088/0004-637x/696/2/2170.

[29] Wiita P J, Quasi-periodic oscillations in the X-ray light curves of Blazars, *Journal of Astrophysics and Astronomy*, 32(1–2) (2011) 147–154. ISSN 0973-7758. https://doi.org/10.1007/s12036-011-9071-y.

[30] Sandrinelli A, Covino S, Treves A, Holgado A M, Sesana A, Lindfors E & Ramazani V F, Quasi-periodicities of BL Lac objects and their origin. https://doi.org/10.48550/ARXIV.1801.06435.

[31] Sukharev A L, Ryabov M I & Bezrukovs V V, Property study of OJ 287 and BL LAC variability in optical and radio ranges, *Radio Physics and Radio Astronomy*, 24(4) (2019) 254. ISSN 2415-7007. https://doi.org/10.15407/rpra24.04.254.

[32] Covino S, Sandrinelli A & Treves A, Gamma-ray quasi-periodicities of Blazars. a cautious approach, *Monthly Notices of the Royal Astronomical Society*, 482(1) (2019) 1270–1274. ISSN 1365-2966. https://doi.org/10.1093/mnras/sty2720.

[33] Vaughan S, A simple test for periodic signals in red noise, *Astronomy & Astrophysics*, 431(1) (2005) 391–403. ISSN 1432-0746. https://doi.org/10.1051/0004-6361:20041453.

[34] Klein-Wolt M & Klis M V D, Identification of Black Hole power spectral components across all canonical states, *The Astrophysical Journal*, 675(2) (2008) 1407. ISSN 1538-4357. https://doi.org/10.1086/525843.

[35] Ingram A & Motta S, A review of quasi-periodic oscillations from Black Hole X-ray binaries: observation and theory, *New Astronomy Reviews* (2019) 101524. https://doi.org/10.48550/ARXIV.2001.08758.